On Qualitative Research of Lattice Dynamical System of Two- and Three-Dimensional Biopixels Array

Vasyl Martsenyuk, Mikolaj Karpinski, Aleksandra Klos-Witkowska, and Andriy Sverstiuk

Abstract We consider the model of two- or three-dimensional biopixels array, which can be used for the design of biosensors. The model is based on the system of lattice differential equations with time delay, describing interactions of biological species of neighboring pixels. The qualitative analysis includes permanence and extinction of solutions, stability investigation, bifurcations, and transition to chaos. The stability conditions are obtained with help of the method of Lyapunov functionals. They are formulated in terms of the value of time necessary for immune response. Numerical research is presented with the help of phase portraits, square and hexagonal lattice plots, and bifurcation diagrams.

Keywords Lattice differnetial equations · Delay · Stability · Biopixel · Extinction · Phase plot

1 Introduction

Nowadays, reaction-diffusion models are used in designing and studies of a lot of detecting, measuring, and sensing devices. One of the examples is the immunosensor which is studied here. Such spatial-temporal models are described by the systems of partial or lattice differential equations.

V. Martsenyuk (✉) · M. Karpinski · A. Klos-Witkowska
University of Bielsko-Biala, 2 Willowa St, 43-309 Bielsko-Biala, Poland
e-mail: vmartsenyuk@ath.bielsko.pl

M. Karpinski
e-mail: mkarpinski@ath.bielsko.pl

A. Klos-Witkowska
e-mail: awitkowska@ath.bielsko.pl

A. Sverstiuk
Ternopil National Medical University, Voli Square 1, Ternopil 46001, Ukraine
e-mail: sverstyuk@tdmu.edu.ua

A. Domoshnitsky et al. (eds.), *Functional Differential Equations and Applications*,
Springer Proceedings in Mathematics & Statistics 379,
https://doi.org/10.1007/978-981-16-6297-3_14

The biosensor models are traditionally studied from the viewpoint of their qualitative analysis. Even in case of a small number of spatial elements, they show complex behavior. In [1], it was shown that the model describes the chemical reaction of two morphogens (reactants), one of them diffusing within two compartments, results in "bi-chaotic" behavior. The origin of such chaotic phenomena[1] were also explained with the help of statistics of topological defects [2].

When considering continuously distributed reaction-diffusion models described by nonlinear partial differential equations, FeigenbaumSharkovskiiMagnitskii bifurcation theory can be applied, which results in a subharmonic cascade of bifurcations of stable limit cycles [3].

The lattice differential equations describe the systems with the discrete spatial structure, which is more consistent with pixel devices. These equations were also called earlier by a series of authors as spatially discrete differential equations [4].

Due to [5], a typical lattice differential equation takes the form

$$\dot{u_\xi} = g_\xi(\{u_\zeta\}_{\zeta\in\Lambda}), \xi \in \Lambda, \tag{1}$$

where we consider a lattice $\Lambda \subset \mathbb{R}^n$, which can be presented as a discrete subset of $\mathbb{R}^n$, consisting of either finite or infinite number of points, which are located in accordance with some regular spatial structure. The vectors $u_\xi, \xi \in \Lambda$ are the values of the state $u = \left\{u_\xi\right\}_{\xi\in\Lambda}$, calculated at the points of the lattice, and g_ξ are the right sides of the equations with the properties enabling us the solution existence.

As a rule, without loss of generality, they consider $\Lambda = \mathbb{Z}^n$, which is the integer lattice in $\mathbb{R}^n$. The methods developed can be easily applied to different types of lattices, namely, the planar rectangular and hexagonal lattice, the crystallographic lattices in $\mathbb{R}^3$.

They pay attention to the notion of delay in lattice differential equations, so-called delayed lattice differential equations. One of the applications dealing with them is the investigation of traveling wavefronts and their stability [5]. The main results are applied to the delayed and discretely diffusive models for the population (see, e.g., [6, 7]).

Lattice differential equations are used as models in a lot of applications, for example, cellular neural networks, image processing, chemical kinetics, material science, in particular, metallurgy and biology [5, 8]. Lattice models are extremely attractive from the viewpoint of population dynamics, especially in case of spatially separated populations [5, 6, 8–11].

There are few reasons requiring consideration of the hexagonal grid instead of rectangular ones (primarily in image and vision computing). Namely, the equal distances between neighboring pixels for hexagonal coordinate systems [12]; hexagonal points are packed more densely [13]; since the "hexagons are 'rounder' than squares", the presentation of curves are more consistent with help of hexagonal systems [13]; hence mathematical operations of edge detection and shape extraction are more successful when applying hexagonal lattices [14].

[1] They call it as "spiral turbulence" [2].

With the purpose of indexing hexagonal pixels, as a rule, they use two-[2] or three-element[3] coordinate systems [15]. Our reasoning will be based on the last one. In contrary to skewed axes, the use of the cubic coordinates enables us symmetries with respect to all three axes.

2 Lattice Model of Antibody–Antigen Interaction for Two-Dimensional Biopixels Array

Let $V_{i,j}(t)$ be the concentration of antigens, $F_{i,j}(t)$ be the concentration of antibodies in biopixel (i, j), $i, j = \overline{1, N}$.
The model is based on the following biological assumptions for arbitrary biopixel (i, j).

1. We have some constant birthrate $\beta > 0$ for antigen population.
2. Antigens are detected, binded, and finally neutralized by antibodies with some probability rate $\gamma > 0$.
3. We have some constant death rate of antibodies $\mu_f > 0$.
4. We assume that when the antibody colonies are absent, the antigen colonies are governed by the well-known delay logistic equation

$$\frac{dV_{i,j}(t)}{dt} = (\beta - \delta_v V_{i,j}(t-\tau))V_{i,j}(t), \tag{2}$$

   where β and δ_v are positive numbers and $\tau \geq 0$ denotes delay in the negative feedback of the antigen colonies.
5. The antibody decreases the average growth rate of antigen linearly with a certain time delay τ; this assumption corresponds to the fact that antibodies cannot detect and bind antigen instantly; antibodies have to spend τ units of time before they are capable of decreasing the average growth rate of the antigen colonies; these aspects are incorporated in the antigen dynamics by the inclusion of the term $-\gamma F_{i,j}(t-\tau)$, where γ is a positive constant which can vary depending on the specific colonies of antibodies and antigens.
6. In the absence of antigen colonies, the average growth rate of the antibody colonies decreases exponentially due to the presence of $-\mu_f$ in the antibody dynamics and so as to incorporate the negative effects of antibody crowding, we have included the term $-\delta_f F_{i,j}(t)$ in the antibody dynamics.
7. The positive feedback $\eta\gamma V_{i,j}(t-\tau)$ in the average growth rate of the antibody has a delay since mature adult antibodies can only contribute to the production of antibody biomass; one can consider the delay τ in $\eta\gamma V_{i,j}(t-\tau)$ as a delay in antibody maturation.

[2] So called "skewed-axis" coordinate system.

[3] It is also known as "cube hex coordinate system".

8. While the last delay need not be the same as the delay in the hunting term and in the term governing antigen colonies, we have retained this for simplicity. We remark that the delays in the antibody term, antibody replacement term, and antigen negative feedback term can be made different and a similar analysis can be followed.
9. We have some diffusion of antigens from four neighboring pixels $(i-1, j)$, $(i+1, j)$, $(i, j-1)$, $(i, j+1)$ (see Fig. 1) with diffusion $D > 0$. Here we consider only diffusion of antigens because the model describes the so-called "competitive" configuration of immunosensor [16]. When considering competitive configuration of immunosensor, the factors immobilized on the biosensor matrix are antigens, while the antibodies play the role of analytes or particles to be detected.
10. We consider surface lateral diffusion (movement of molecules on the surface on solid phase toward immobilizated molecules) [17]. Moreover, there are works [18, 19] which assume and consider surface diffusion as an entirely independent stage.
11. We extend the definition of the usual diffusion operator in case of surface diffusion in the following way. Let $n \in (0, 1]$ be a factor of diffusion disbalance. It means that only nth portion of antigens of the pixel (i, j) may be included in the diffusion process to any neighboring pixel as a result of surface diffusion.

For the reasoning given, we consider a very simple delayed antibody–antigen competition model for biopixels two-dimensional array, which is based on well-known Marchuk model [20–23] and using spatial operator $\hat{S}$ offered in [24] (Supplementary information, p. 10)

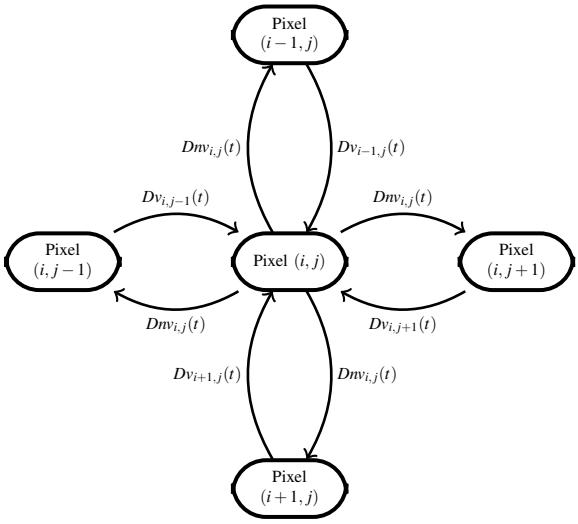

Fig. 1 Linear lattice interconnected four neighboring pixels model, $n > 0$ is disbalance constant

$$\begin{aligned}\frac{dV_{i,j}(t)}{dt} &= (\beta - \gamma F_{i,j}(t-\tau) - \delta_v V_{i,j}(t-\tau))V_{i,j}(t) + \hat{S}\{V_{i,j}\},\\ \frac{dF_{i,j}(t)}{dt} &= (-\mu_f + \eta\gamma V_{i,j}(t-\tau) - \delta_f F_{ij}(t))F_{i,j}(t)\end{aligned} \tag{3}$$

with given initial functions

$$\begin{aligned}&V_{i,j}(t) = V^0_{i,j}(t) \geq 0, \quad F_{i,j}(t) = F^0_{i,j}(t) \geq 0, \quad t \in [-\tau, 0),\\ &V_{i,j}(0), F_{i,j}(0) > 0.\end{aligned} \tag{4}$$

For a square $N \times N$ array of traps, we use the following discrete diffusion form of the spatial operator [24]

$$\hat{S}\{V_{i,j}\} = \begin{cases} D\left[V_{1,2} + V_{2,1} - 2nV_{1,1}\right] & i, j = 1\\ D\left[V_{2,j} + V_{1,j-1} + V_{1,j+1} - 3nV_{i,j}\right] & i = 1, j \in \overline{2, N-1}\\ D\left[V_{1,N-1} + V_{2,N} - 2nV_{1,N}\right] & i = 1, j = N\\ D\left[V_{i-1,N} + V_{i+1,N} + V_{i,N-1} - 3nV_{i,N}\right] & i =\in \overline{2, N-1}, j = N\\ D\left[V_{N-1,N} + V_{N,N-1} - 2nV_{N,N}\right] & i = N, j = N\\ D\left[V_{N-1,j} + V_{N,j-1} + V_{N,j+1} - 3nV_{N,j}\right] & i = N, j \in \overline{2, N-1}\\ D\left[V_{N-1,1} + V_{N,2} - 2nV_{N,1}\right] & i = N, j = 1\\ D\left[V_{i-1,1} + V_{i+1,1} + V_{i,2} - 3nV_{i,1}\right] & i \in \overline{2, N-1}, j = 1\\ D\left[V_{i-1,j} + V_{i+1,j} + V_{i,j-1} + V_{i,j+1} - 4nV_{i,j}\right] & i, j \in \overline{2, N-1}\end{cases} \tag{5}$$

Each colony is affected by the antigen produced in four neighboring colonies, two in each dimension of the array, separated by the equal distance Δ. We use the boundary condition $V_{i,j} = 0$ for the edges of the array $i, j = 0, N+1$. Further, we will use the following notation of the constant

$$k(i,j) = \begin{cases} 2 & i, j = 1; \quad i = 1, j = N; \quad i = N, j = N; \quad i = N, j = 1,\\ 3 & i = 1, j \in \overline{2, N-1}; \quad i \in \overline{2, N-1}, j = N; \quad i = N, j \in \overline{2, N-1};\\ & i \in \overline{2, N-1}, j = 1\\ 4 & i, j \in \overline{2, N-1}\end{cases} \tag{6}$$

which will be used in manipulations with the spatial operator (20).

Results of modeling (3) are presented further. It can be seen that the qualitative behavior of the system is determined mostly by the time of immune response τ (or time delay), diffusion D, and constant n.

2.1 Stability Investigation

2.1.1 Steady States

The steady states of the model (3) are the intersection of the null-clines $dV_{i,j}(t)/dt = 0$ and $dF_{i,j}(t)/dt = 0, i, j = \overline{1, N}$.

Antigen-free steady state. If $V_{i,j}(t) \equiv 0$, the free antigen equilibrium is at $\mathscr{E}^0_{i,j} \equiv \Big(0, 0\Big), i, j = \overline{1, N}$ or $\mathscr{E}^0_{i,j} \equiv \Big(0, -\frac{\mu_f}{\delta_f}\Big), i, j = \overline{1, N}$. The last solution does not have biological sense and cannot be reached for nonnegative initial conditions (19).

When considering endemic steady state $\mathscr{E}^*_{i,j} \equiv \Big(V^*_{i,j}, F^*_{i,j}\Big), i, j = \overline{1, N}$ for (3) we get algebraic system:

$$\begin{aligned} &\Big(\beta - \gamma F^*_{i,j} - \delta_v V^*_{i,j}\Big) V^*_{i,j} + \hat{S}\left\{V^*_{i,j}\right\} = 0, \\ &\Big(-\mu_f + \eta\gamma V^*_{i,j} - \delta_f F^*_{i,j}\Big) F^*_{i,j} = 0, \quad i, j = \overline{1, N}. \end{aligned} \tag{7}$$

The solutions $\Big(V^*_{i,j}, F^*_{i,j}\Big)$ of (7) can be found as a result of solving lattice equation with respect to $V^*_{i,j}$, and using relation $F^*_{i,j} = \frac{-\mu_f + \eta\gamma V^*_{i,j}}{\delta_f}$

Thus we have to differ two cases.

Identical endemic state for all pixels. Let's assume there is the solution of (7) $V^*_{i,j} \equiv V^*$, $F^*_{i,j} \equiv F^*$, $i, j = \overline{1, N}$, i.e., $\hat{S}\left\{V^*_{i,j}\right\} \equiv 0$. Then $\mathscr{E}^*_{i,j} = \Big(V^*, F^*\Big)$, $i, j = \overline{1, N}$ can be calculated as

$$V^* = \frac{-\beta\delta_f - \gamma\mu_f}{\delta_v\delta_f - \eta\gamma^2}, \quad F^* = \frac{\delta_v\mu_f - \eta\gamma\beta}{\delta_v\delta_f - \eta\gamma^2}. \tag{8}$$

provided that $\delta_v\delta_f - \eta\gamma^2 < 0$.

Nonidentical endemic state for pixels. In the general case, we have an endemic steady state which is different from (8). It is shown numerically in Appendix B that it appears as a result of diffusion between pixels D.

At the absence of diffusion, i.e., $D = 0$, we have only an identical endemic state for pixels of external layer. At the presence of diffusion,i.e., $D > 0$, nonidentical endemic states tends to be identical ones (8) at internal pixels, which can be observed at numerical simulation. This phenomenon clearly appears at bigger amount of pixels.

Basic reproduction numbers. Here we define the basic reproduction number for antigen colony which is localized in pixel (i, j). When considering epidemic models, the basic reproduction number, $\mathscr{R}_0$, is defined as the expected number of secondary cases produced by a single (typical) infection in a completely susceptible population. It is important to note that $\mathscr{R}_0$ is a dimensionless number [25]. When applying this definition to the pixel (i, j), which is described by the Eq. (3), we get

$$\mathscr{R}_{0,i,j} = \mathscr{T}_{i,j}\overline{c}_{i,j}, d_{i,j}$$

where $\mathscr{T}_{i,j}$ is the transmissibility (i.e., probability of binding given constant between an antigen and antibody), $\overline{c}_{i,j}$ is the average rate of contact between antigens and antibodies, and $d_{i,j}$ is the duration of binding of antigen by antibody till deactivation.

Unfortunately, the lattice system (3) doesn't include all parameters, which allows to calculate the basic reproduction numbers in a clear form. Firstly, let's consider pixel $(i^\star, j^\star)$ without diffusion, i.e., $\hat{S}\left\{V_{i^\star,j^\star}\right\} \equiv 0$. In this case, the non-negative equilibria of (3) are

$$\mathscr{E}^0_{i^\star,j^\star} = \left(V^0, 0\right) := \left(\frac{\beta}{\delta_v}, 0\right), \quad \mathscr{E}^\star_{i^\star,j^\star} = \left(V^\star, F^\star\right).$$

Due to the approach which was offered in [26] (in pages 4 for ordinary differential equations, 5 for delay model), we introduce the basic reproduction number for pixel $(i^\star, j^\star)$ without diffusion, which is given by expression

$$\mathscr{R}_{0,i^\star,j^\star} := \frac{V^0}{V^\star} = \frac{\beta}{\delta_v V^\star} = \frac{\beta(\eta\gamma^2 - \delta_v\delta_f)}{\delta_v(\beta\delta_f + \gamma\mu_f)}.$$

Its biological meaning is given as being the average number of offsprings produced by a mature antibody in its lifetime when introduced in an antigen-only environment with antigen at carrying capacity.

According to the common theory, it can be shown that antibody-free equilibrium $\mathscr{E}^0_{i^\star,j^\star}$ is locally asymptotically stable if $\mathscr{R}_{0,i^\star,j^\star} < 1$ and it is unstable if $\mathscr{R}_{0,i^\star,j^\star} > 1$. It can be done with help of analysis of the roots of characteristic equation (similarly to [26], p. 5). Thus, $\mathscr{R}_{0,i^\star,j^\star} > 1$ is sufficient condition for existence of the endemic equilibrium $\mathscr{E}^\star_{i^\star,j^\star}$.

We can consider the expression mentioned above for the general case of the lattice system (3), i.e., when considering diffusion. In this case, we have the "lattice" of the basic reproduction numbers $\mathscr{R}_{0,i,j}$, $i, j = \overline{1, N}$ satisfying to

$$\mathscr{R}_{0,i,j} := \frac{V^0_{i,j}}{V^\star_{i,j}}, \quad i, j = \overline{1, N}, \tag{9}$$

where $\mathscr{E}^0_{i,j}$, $i, j = \overline{1, N}$ are nonidentical steady states, which are found as a result of solution of the algebraic system

$$\left(\beta - \delta_v V^0_{i,j}\right)V^0_{i,j} + \hat{S}\left\{V^0_{i,j}\right\} = 0, \quad i, j = \overline{1, N}, \tag{10}$$

endemic states $\mathscr{E}^\star_{i,j} = \left(V^\star_{i,j}, F^\star_{i,j}\right)$, $i, j = \overline{1, N}$ are found using (7).

It is worth to say that due to the common theory the conditions

$$\mathscr{R}_{0,i,j} > 1, \quad i, j = \overline{1, N} \tag{11}$$

are sufficient for the existence of endemic state $\mathscr{E}^{\star}_{i,j}$. We will check it only with help of numerical simulations.

2.2 Persistence of the Solutions

We will use the following definition which generalizes [27] for lattice differential equations.

Definition 1 System (3) is said to be uniformly persistent if for all $i, j = \overline{1, N}$ there exist compact regions $\mathscr{D}_{i,j} \subset \text{int}\, \mathbb{R}^2$ such that every solution $(V_{i,j}(t), F_{i,j}(t))$, $i, j = \overline{1, N}$ of (3) with the initial conditions (19) eventually enters and remains in the region $\mathscr{D}_{i,j}$.

Theorem 1 *Let $(V_{i,j}(t), F_{i,j}(t))$, $i, j = \overline{1, N}$ be the solutions of (3) with initials conditions (19). If*

$$\beta\eta\gamma - \mu_f\delta_v > 0, \tag{12}$$

then

$$0 < V_{i,j}(t) \le M_v, \quad 0 < F_{i,j}(t) \le M_f \tag{13}$$

for some large values of t. Here

$$M_v = \frac{\beta}{\delta_v} e^{\beta\tau}, \quad M_f = \frac{1}{\delta_f}\Big(\eta\gamma M_v - \mu_f\Big). \tag{14}$$

Proof Firstly, we can prove that there exists some large instant of time T_1 that $\hat{S}\{V_{i,j}(t)\} \le 0$, $i, j = \overline{1, N}$, $t > T_1$.

Let's assume the contrary, i.e., there is $i^{\star}$, $j^{\star} \in \overline{1, N}$, that $\hat{S}\{V_{i,j}(t)\} > 0$ at $t > T_1$, which is a contradiction with a balance principle.

Since the solutions of the system (3), (19) are positive, then

$$\frac{dV_{i,j}(t)}{dt} \le \Big(\beta - \delta_v V_{i,j}(t-\tau)\Big)V_{i,j}(t). \tag{15}$$

Further, we can apply the basic steps of proof of Lemma 3.1 [28] which is proved in nonlattice case (i.e., without spatial operator).

Remark 1 Conditions of uniform persistence of system (3) in nonlattice case were obtained in [29]. They resulted in inequality (12) provided that

$$\beta\delta_f + \mu_f\gamma > 0 \tag{16}$$

holds.

2.3 Extinction Research

The next result introduces a sufficient condition for the underlying grid size ensuring that the solution of (3) is non-vanishing.

Theorem 2 *Let for the system (3) the positive orthant Ω be positive invariant. Besides that, let N be such that $f_{extnc}(N) < 1$ holds, where*

$$f_{extnc}(N) = \max_{k,l=\overline{1,N}} \left| \beta - \frac{4D}{\Delta^2} \left(1 + \cos \frac{\pi(k+l)}{2(N+1)} \cos \frac{\pi(k-l)}{2(N+1)} \right) \right|. \tag{17}$$

Then $\lim_{t\to\infty} V_{i,j}(t) = 0$, $i, j = \overline{1, N}$.

Proof It requires a comparison principle for differential equations.

The following inequalities hold for $V_{i,j}(t)$

$$\frac{V_{i,j}(t)}{dt} < \beta V_{i,j}(t) + \hat{S}\left\{V_{i,j}(t)\right\}.$$

Consider N^2-vector of the form

$$V(n) = \Big(V_{1,1}(t), V_{1,2}(t), \ldots, V_{1,N}(t), V_{2,1}(t), \ldots, V_{2,N}(t), \ldots, V_{N,1}(t), \ldots, V_{N,N}(t) \Big)^{\top}.$$

We compare $\frac{V(t)}{dt} \le CV(t)$, where $C = I_N \otimes A + B \otimes I_N$,

$$A = \begin{bmatrix} \beta - \frac{4D}{\Delta^2} & \frac{D}{\Delta^2} & & & & \\ \frac{D}{\Delta^2} & \beta - \frac{4D}{\Delta^2} & \frac{D}{\Delta^2} & & & \\ & \frac{D}{\Delta^2} & \ddots & & & \\ & & & \ddots & & \\ & & & & \beta - \frac{4D}{\Delta^2} & \frac{D}{\Delta^2} \\ & & & & \frac{D}{\Delta^2} & \beta - \frac{4D}{\Delta^2} \end{bmatrix} \in \mathbb{R}^{N\times N},$$

$$B = \begin{bmatrix} 0 & \frac{D}{\Delta^2} & & & & \\ \frac{D}{\Delta^2} & 0 & \frac{D}{\Delta^2} & & & \\ & \frac{D}{\Delta^2} & \ddots & & & \\ & & & \ddots & & \\ & & & & 0 & \frac{D}{\Delta^2} \\ & & & & \frac{D}{\Delta^2} & 0 \end{bmatrix} \in \mathbb{R}^{N\times N},$$

I_N is $N \times N$ identity matrix. The N^2 eigenvalues of C are of the form (see [30], Theorem 8.3.1) $\lambda_{k,l}(C) = \lambda_k(A) + \lambda_l(B)$, $k, l = \overline{1, N}$, where the eigenvalues of A

$$\lambda_k(A) = \beta - \frac{4D}{\Delta^2} - \frac{2D}{\Delta^2} \cos\left(\pi k/(N+1)\right), \quad k = \overline{1, N},$$

the eigenvalues of B

$$\lambda_l(B) = -\frac{2D}{\Delta^2} \cos\left(\pi l/(N+1)\right), \quad l = \overline{1, N}.$$

The comparison system $\frac{Z(t)}{dt} = CZ(t)$ tends asymptotically to zero if $\left|\lambda_{k,l}\right| < 1$. That is

$$\max_{k,l=\overline{1,N}} \left| \beta - \frac{4D}{\Delta^2} - \frac{2D}{\Delta^2} \left(\cos \frac{\pi k}{N+1} + \cos \frac{\pi l}{N+1} \right) \right| < 1.$$

2.4 *Numerical Simulation of Square* 4 × 4 *Pixels Array*

First of all, we calculate the basic reproductive numbers $\mathscr{R}_{0,i,j}$, $i, j = \overline{1, 4}$ due to (9) (See Table 1). We see that the conditions (11) hold. Thus, equilibrium without antibodies $\mathscr{E}^0_{i,j}$, $i, j = \overline{1, 4}$ is unstable and there exists endemic equilibrium $\mathscr{E}^\star_{i,j}$, $i, j = \overline{1, 4}$.

The numerical simulations were implemented at different values of $n \in (0, 1]$. Here we can see that when changing the value of τ we have changes in the qualitative behavior of pixels and the entire immunosensor. We considered the parameter value set given above and computed the long-time behavior of the system (3) for $\tau = 0.05, 0.22, 0.23, 0.2865$, and 0.28725. The phase diagrams of the antibody versus antigen populations for the pixel $(1, 1)$ are shown in Table 2.

For example, at $\tau \in [0, 0.22]$, we can see trajectories corresponding to the stable node for all pixels.

For $\tau = 0.23$, the phase diagrams show that the solution is a limit cycle with two local extrema (one local maximum and one local minimum) per cycle. Then for $\tau = 0.2825$, the solution is a limit cycle with four local extrema per cycle, and,

Table 1 The values of $R_{0,i,j}$, $i, j = \overline{1, 4}$

$R^\star_{0,i,j}$	1	2	3	4
1	3.218727	3.425273	3.474323	3.224824
2	3.171270	3.235043	3.236289	3.126438
3	3.092287	3.107824	3.096617	3.040443
4	2.997269	3.020902	3.012915	2.971442

Table 2 The phase plane plots of the system (3) for antibody populations $F_{i,j}$ versus antigen populations $V_{i,j}$, $i, j = \overline{1,4}$. Numerical simulation of the system (3) at $n = 0.9, \tau = 0.28725$. Here • indicates identical steady state, • indicates nonidentical steady state. Trajectories are constructed for $t \in [550, 800]$. The solution behavior looks chaotic

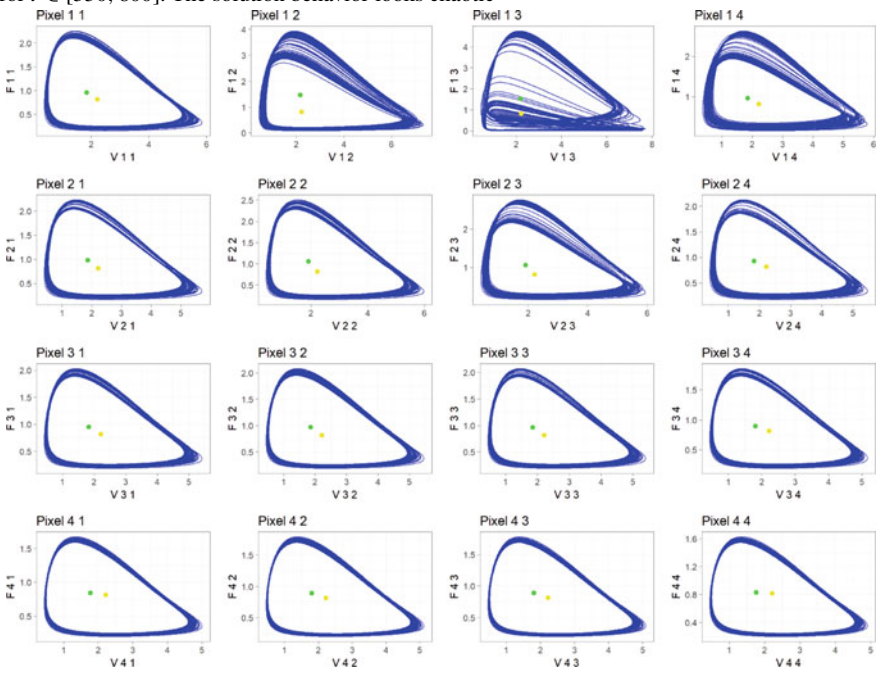

for $\tau = 0.2868, 0.2869, 0.28695$ the solutions are limit cycles with 8, 16, and 32 local extrema per cycle, respectively. Finally, for $\tau = 0.28725$, the behavior shown in Table 2 is obtained which looks like chaotic behavior. In this paper, we have regarded behavior as chaotic if no periodic behavior could be found in the long-time behavior of the solutions.

As a check that the solution is chaotic for $\tau = 0.28725$, we perturbed the initial conditions to test the sensitivity of the system. Figure 2 shows a comparison of the solutions for the antigen population $V_{1,3}$ with initial conditions $V_{1,3}(t) = 1$ and $V_{1,3}(t) = 1.001$, $t \in [-\tau, 0]$, and identical all the rest ones. Near the initial time, the two solutions appear to be the same, but as time increases, there is a marked difference between the solutions supporting the conclusion that the system behavior is chaotic at $\tau = 0.28725$.

We have also checked numerically that the solutions for the limit cycles are periodic and computed the periods for each of the local maxima and minima in the cycles. In the chaotic solution region, the numerical calculations (not shown in this paper) confirmed that no periodic behavior could be found.

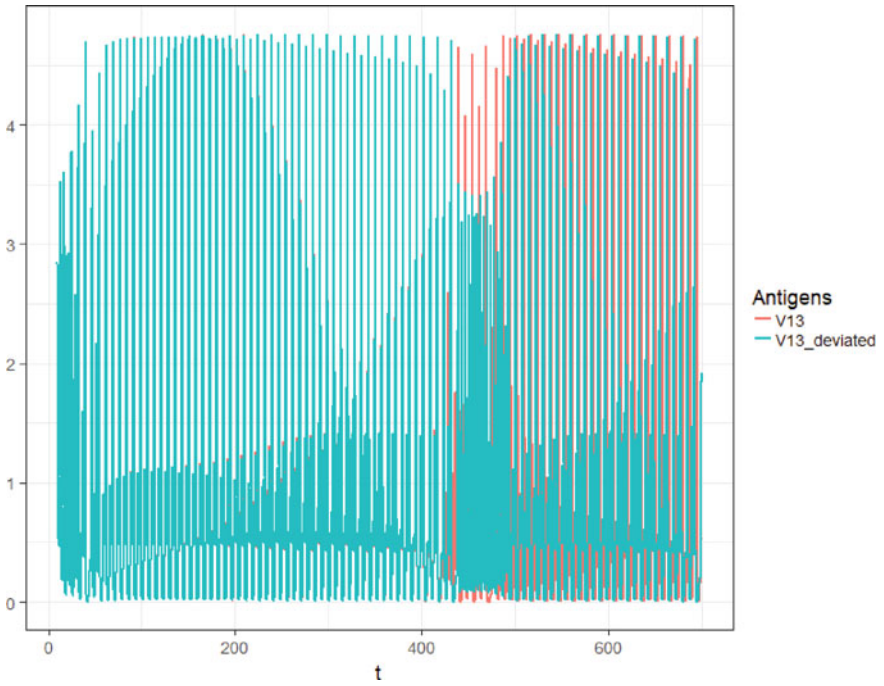

Fig. 2 The time series of the solutions to the system (3) for the antigen population $V_{1,3}$ from $t = 0$ to 700 with $\tau = 0.28725$ for initial conditions $V_{1,3}(t) = 1$ and $V_{1,3}(t) = 1.001$ (deviated), $t \in [-\tau, 0]$, and identical all the rest ones. At the beginning, the two solutions appear to be the same, but as time increases there is a marked difference between the solutions supporting the conclusion that the system behavior is chaotic

A bifurcation diagram showing the maximum and minimum points for the limit cycles for the antigen population $V_{1,3}$ as a function of time delay is given in Fig. 3. The Hopf bifurcation from the stable equilibrium point to a simple limit cycle and the sharp transitions at critical values of the time delay between limit cycles with increasing numbers of maximum and minimum points per cycle can be clearly seen.

3 Three-Dimensional Biopixels Array

When modeling three-dimensional pixels array, it is natural way to apply the model based on the hexagonal lattice. Such model may use the following assumption. Namely, antigens are assumed to diffuse from six neighboring pixels, $(i + 1, j, k - 1)$, $(i + 1, j - 1, k)$, $(i, j - 1, k + 1)$, $(i - 1, j, k + 1)$, $(i - 1, j + 1, k)$, $(i, j + 1, k - 1)$ (see Fig. 1), with diffusion rate $D\Delta^{-2}$, where $D > 0$ and $\Delta > 0$ is distance between pixels.

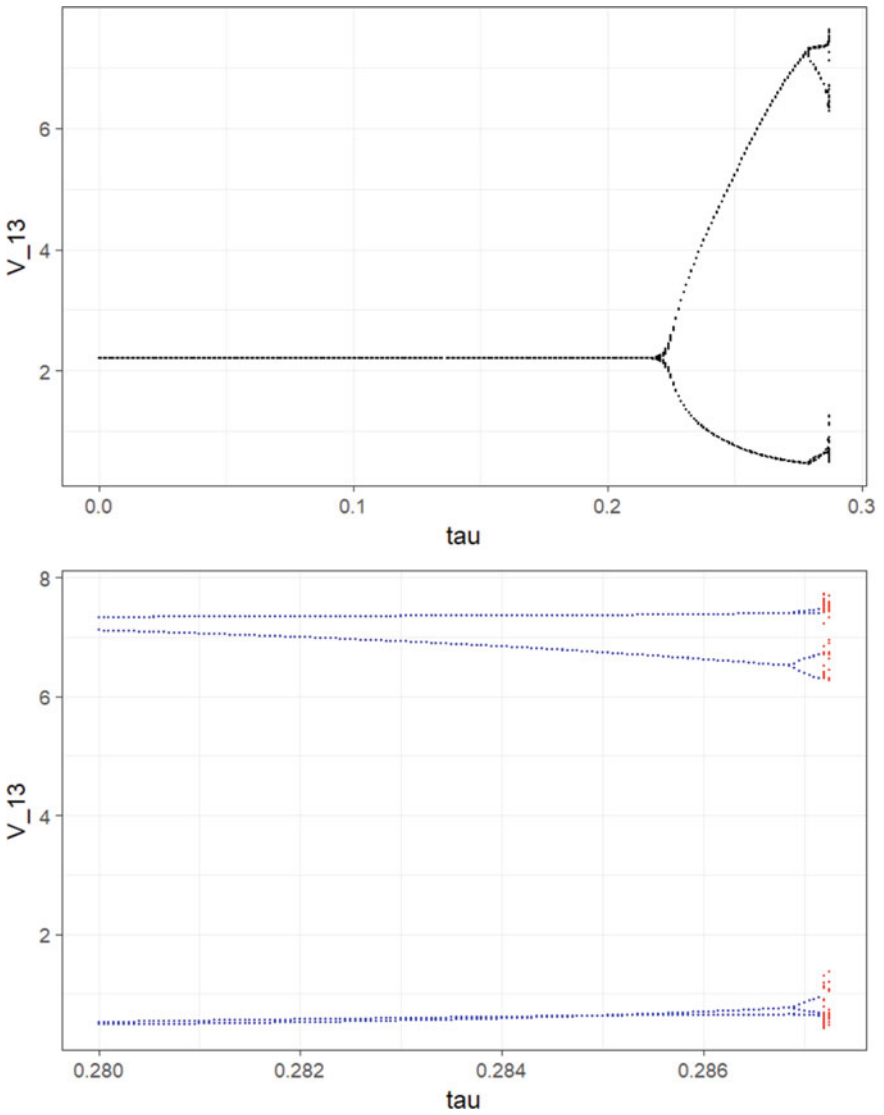

Fig. 3 A bifurcation diagram showing the "bifurcation path to chaos" as the time delay is increased. The points show the local extreme points per cycle for the $V_{1,3}$ population. Chaotic-type solutions occur at $\tau \approx 0.28725$ and are indicated in red in the figure with value 0 for the number of extreme points

Taking into account prerequisites mentioned above, we get a simplified antibody–antigen competition model with delay for a hexagonal array of biopixels, which uses Marchuk model of the immune response [20–23] and using spatial operator $\hat{S}$ which is constructed similarly to [24] (Supplementary information, p. 10)

$$\begin{aligned}\frac{dV_{i,j,k}(t)}{dt} &= (\beta - \gamma F_{i,j,k}(t-\tau) - \delta_v V_{i,j,k}(t-\tau))V_{i,j,k}(t) + \hat{S}\{V_{i,j,k}\},\\ \frac{dF_{i,j,k}(t)}{dt} &= (-\mu_f + \eta\gamma V_{i,j,k}(t-\tau) - \delta_f F_{i,j,k}(t))F_{i,j,k}(t)\end{aligned} \tag{18}$$

with given initial functions

$$\begin{aligned}&V_{i,j,k}(t) = V^0_{i,j,k}(t) \geq 0, \quad F_{i,j,k}(t) = F^0_{i,j,k}(t) \geq 0, \quad t \in [-\tau, 0),\\ &V_{i,j,k}(0), F_{i,j,k}(0) > 0.\end{aligned} \tag{19}$$

We use the following spatial operator of discrete diffusion for a hexagonal array of pixels[4]

$$\begin{aligned}\hat{S}\{V_{i,j,k}\} = D\Delta^{-2}\Big[&V_{i+1,j,k-1} + V_{i+1,j-1,k} + V_{i,j-1,k+1} + V_{i-1,j,k+1} + V_{i-1,j+1,k}\\ &+ V_{i,j+1,k-1} - 6nV_{i,j,k}\Big]\\ &i,j,k \in \overline{-N+1, N-1}, \quad i+j+k = 0.\end{aligned} \tag{20}$$

Each pixel is affected by the antigens flowing out six neighboring pixels, two in each of three directions of the hexagonal array. The adjoint pixels are separated by the distance Δ (Fig. 4).

Boundary conditions $V_{i,j,k} = 0$ for the edges of the hexagonal array, i.e., if $i \vee j \vee k \in \{-N-1, N+1\}$, are used.

We can present analytical results with respect to the model (18) in the form of restrictions for the parameters, enabling us persistence and global asymptotic stability. Moreover, we executed numerical research of the system qualitative behavior in dependence of changes of the time of immune response τ (delay of time), diffusion rate $D\Delta^{-2}$ and factor n.

3.1 Persistence and Extinction of Solutions

Concerning persistence, for the hexagonal lattice the similar result can be obtained as for square one (Theorem 1), just adding the third index.

[4] Without loss of generality we consider spatial operator for internal pixels only.

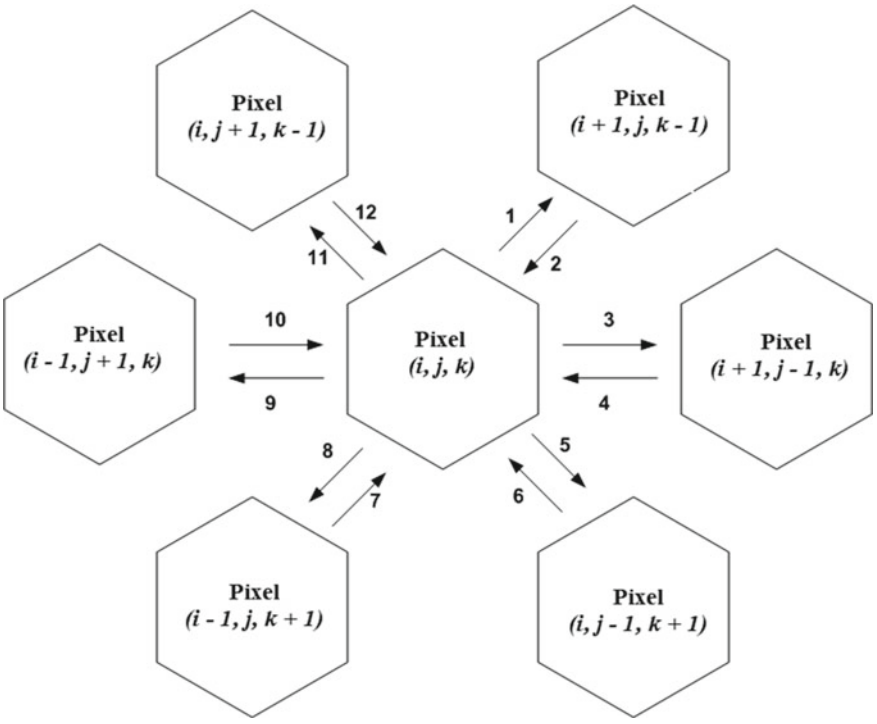

Fig. 4 Diffusion of antigens for the hexagonal lattice model. Antigens from six neighboring pixels interact, $n > 0$ is the constant of disbalance. Here '1', '3', '5', '8', '9', '11' have to be replaced with $D\Delta^{-2}V_{i,j,k}(t)$, '2' with $D\Delta^{-2}V_{i+1,j,k-1}(t)$, '4' with $D\Delta^{-2}V_{i+1,j-1,k}(t)$, '6' with $D\Delta^{-2}V_{i,j-1,k+1}(t)$, '7' with $D\Delta^{-2}V_{i-1,j,k+1}(t)$, '10' with $D\Delta^{-2}V_{i-1,j+1,k}(t)$, '12' with $D\Delta^{-2}V_{i,j+1,k-1}(t)$

Unfortunately, we didn't manage to present such a clear condition of extinction as in Theorem 2. We can check it only numerically in an experimental way.

3.2 Numerical Study

For numerical simulation, we consider model (18) of hexagonal pixels array at $N = 4$, $\beta = 2\ \text{min}^{-1}$, $\gamma = 2\frac{mL}{min\cdot\mu g}$, $\mu_f = 1\ \text{min}^{-1}$, $\eta = 0.8/\gamma$, $\delta_v = 0.5\frac{mL}{min\cdot\mu g}$, $\delta_f = 0.5\frac{mL}{min\cdot\mu g}$, $D = 0.2\frac{nm^2}{min}$, $\Delta = 0.3nm$. Numerical modeling was implemented at different values of $n \in (0, 1]$. For this purpose, we used RStudio environment.

Using local bifurcation plot, dynamics of the system (18) was analyzed for different values of $n \in (0, 1]$. We have concluded that oscillatory and then chaotic behavior starts for smaller values of τ at smaller values of n. Further, increasing the values of n, we can observe asymptotically stable steady solutions for a wider range of τ.

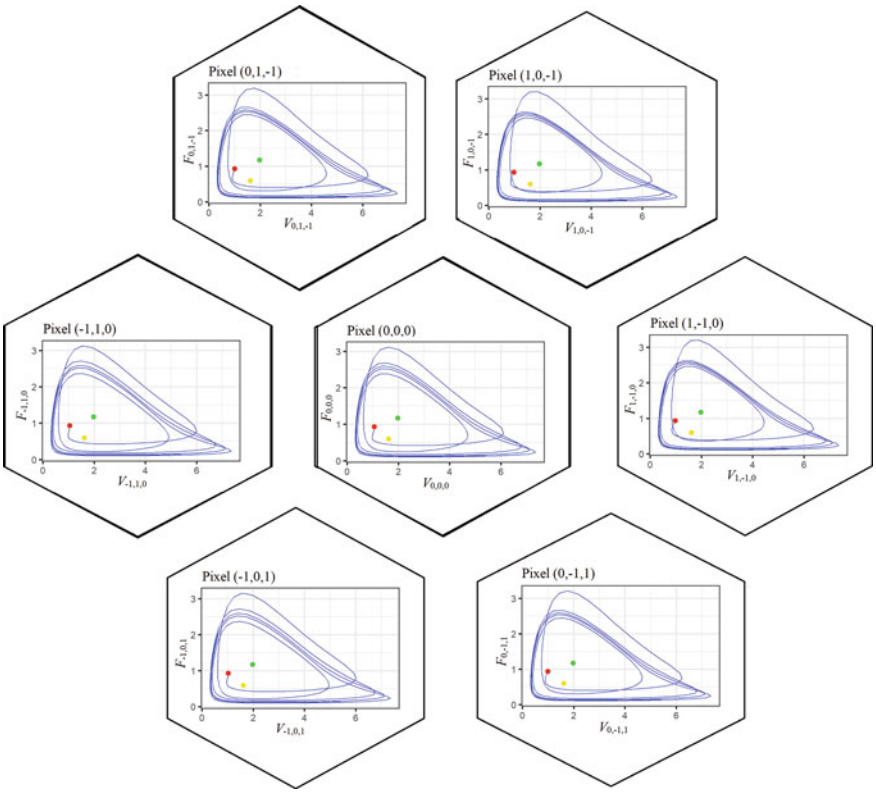

Fig. 5 Phase plots of the system (18) at $\tau = 0.287$. Here • indicates initial state, • indicates pixel-independent endemic state, • indicates pixel-dependent endemic state. The solution tends to a stable limit cycle with six local extrema per cycle

Numerical integration of the system has shown the influence of time delay τ. Namely, as it is agreed with the analytical results, we observe the stable focuses at pixel-dependent endemic states for small delays $\tau \in [0, 0.18)$. At $\tau \approx 0.18$ min the stable focus is transformed into a stable limit cycle of tiny radius, which corresponds to Hopf bifurcation. A deeper study of this phenomenon requires obtaining the condition of the appearance of the pair of purely imaginary roots of the characteristic quasipolynomial of the linearized system. The limit cycles of ellipsoidal form are observed till $\tau \approx 0.285$ min. Pay attention that when increasing τ, near $\tau = 0.285$, we get period doubling (see Fig. 5).[5]

The qualitative behavior of immunosensor model can be analyzed with help of hexagonal tiling plots also. For this purpose, we can use both plots for antigens (Fig. 6), antibodies (Fig. 7), and probabilities of binding antigens by antibodies (Fig. 8).

[5] It can be approximately seen from local bifurcation plot also.

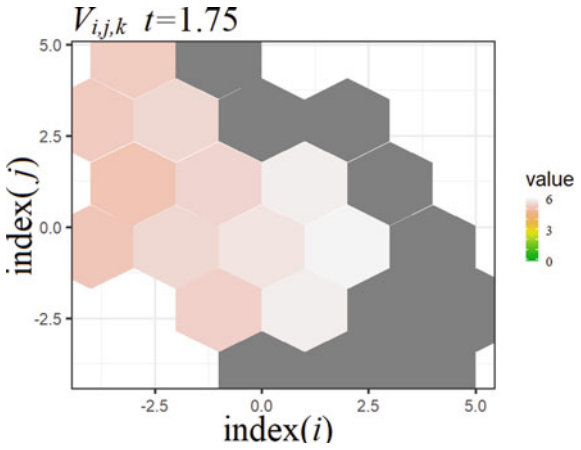

Fig. 6 Example of hexagonal tiling plot for V

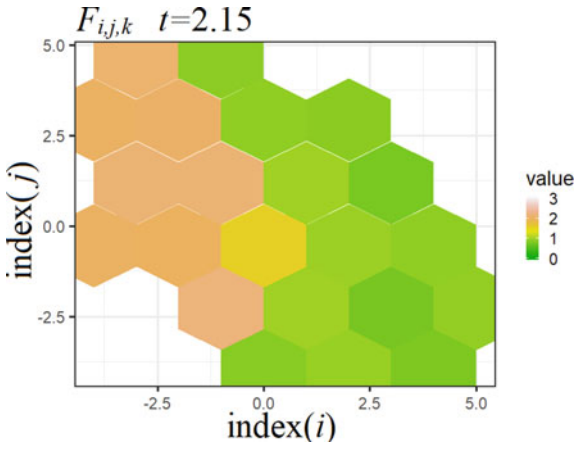

Fig. 7 Example of hexagonal tiling plot for F

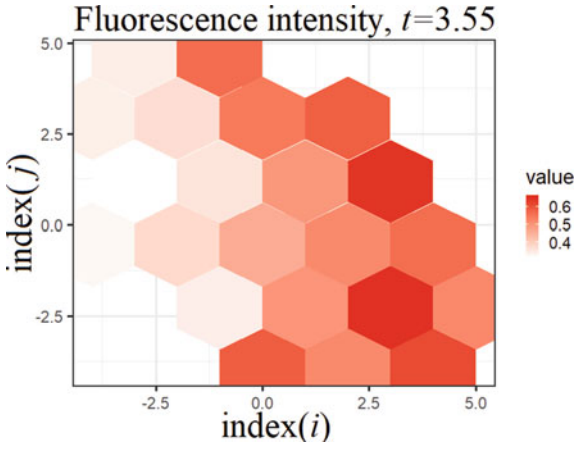

Fig. 8 Example of hexagonal tiling plot for probabilities of binding antigens by antibodies, i.e., $V \times F$. In case of optical immunosensor, it is fluorescence intensity

4 Conclusions

In this work, reaction-diffusion models of two- and three-dimensional immunopixels array were considered. Mathematically, it is described by the system of lattice delayed differential equations on rectangular or hexagonal grids. The systems include the spatial operator describing the diffusion of antigens between pixels.

The main results are dealing with the qualitative investigation of the model. The conditions of persistence were obtained. Also, we have managed to get the result dealing with the extinction of the solutions. Namely, it can be seen that the amount of pixels determines their non-vanishing. In a two-dimensional case, this dependence can be presented in a clear form.

The conditions of local or global asymptotic stability can be obtained using the construction of the Lyapunov functional. Because of the cumbersome evidence, we didn't include it here. They result in inequality including the system parameters and delay. So, estimation of the delay enabling us local or global asymptotic stability can be obtained.

Numerical analysis of the model qualitative behavior is performed with the help of the bifurcation diagram, phase trajectories, and rectangular or hexagonal tile portraits. It has shown the changes in qualitative behavior with respect to the growth of time delay. Namely, starting from the stable focus at small delay values, then through Hopf bifurcation to limit cycles, and finally through period doublings to deterministic chaos. It is agreed with the results on space-time chaos for reaction-diffusion systems, which were previously obtained in [1–3].

As compared with the rectangular lattice model, for the hexagonal model, we observe Hopf bifurcation at smaller values of τ. That is hexagonal lattice accelerates changes in qualitative behavior.

Note, that model can be applied for an arbitrary amount of pixels determined by natural $N \geq 1$. However, it can be numerically seen that qualitative behavior of the entire immunosensor is determined by 5 or 7 pixels array for square and hexagonal lattices, respectively.

Acknowledgements We are very thankful to the reviewers for valuable remarks and comments which allowed us to improve the work.

References

1. Rössler, O.E.: Chemical turbulence: Chaos in a simple reaction-diffusion system. Zeitschrift für Naturforschung A **31**(10) (1976). https://doi.org/10.1515/zna-1976-1006
2. Hildebrand, M., Bar, M., Eiswirth, M.: Statistics of topological defects and spatiotemporal chaos in a reaction-diffusion system. Phys. Rev. Lett. **75**(8), 1503–1506 (1995). https://doi.org/10.1103/physrevlett.75.1503
3. Zaitseva, M.F., Magnitskii, N.A.: Space-time chaos in a system of reaction-diffusion equations. Differ. Equ. **53**(11), 1519–1523 (2017)

4. Cahn, J.W., Chow, S., Van Vleck, E.S.: Spatially discrete nonlinear diffusion equations. Rocky Mount. J. Math., to appear (1995)
5. Chow, S.-N., Mallet-Paret, J., Van Vleck, E.S.: Dynamics of lattice differential equations. Int. J. Bifurc. Chaos **6**(09), 1605–1621 (1996)
6. Pan, S.: Propagation of delayed lattice differential equations without local quasimonotonicity (2014). arXiv:1405.1126
7. Huang, J., Lu, G., Zou, X.: Existence of traveling wave fronts of delayed lattice differential equations. J. Math. Anal. Appl. **298**(2), 538–558 (2004)
8. Niu, H.: Spreading speeds in a lattice differential equation with distributed delay. Turkish J. Math. **39**(2), 235–250 (2015)
9. Hoffman, A., Hupkes, H., Van Vleck, E.: Entire Solutions for Bistable Lattice Differential Equations with Obstacles. American Mathematical Society, Providence (2017)
10. Wu, F.: Asymptotic speed of spreading in a delay lattice differential equation without quasi-monotonicity. Electr. J. Differ. Equ. **2014**(213), 1–10 (2014)
11. Zhang, G.-B.: Global stability of traveling wave fronts for non-local delayed lattice differential equations. Nonlinear Anal.: Real World Appl. **13**(4), 1790–1801 (2012)
12. Luczak, E., Rosenfeld, A.: Distance on a hexagonal grid. IEEE Trans. Comput. **25**(5), 532–533 (1976). https://doi.org/10.1109/TC.1976.1674642
13. Hexagonal coordinate systems. https://homepages.inf.ed.ac.uk/rbf/CVonline/LOCAL_COPIES/AV0405/MARTIN/Hex.pdf. Accessed 12 May 2019
14. Middleton, L., Sivaswamy, J.: Edge detection in a hexagonal-image processing framework. Image Vis. Comput. **19**(14), 1071–1081 (2001)
15. Fayas, A., Nisar, H., Sultan, A.: Study on hexagonal grid in image processing. In: The 4th International Conference on Digital Image Processing, pp. 7–8 (2012)
16. Cruz, H.J., Rosa, C.C., Oliva, A.G.: Immunosensors for diagnostic applications. Parasitol. Res. **88**, S4–S7 (2002)
17. Paek, S.-H., Schramm, W.: Modeling of immunosensors under nonequilibrium conditions: I. Mathematic modeling of performance characteristics. Anal. Biochem. **196**(2), 319–325 (1991)
18. Bloomfield, V., Prager, S.: Diffusion-controlled reactions on spherical surfaces. application to bacteriophage tail fiber attachment. Biophys. J. **27**(3), 447–453 (1979)
19. Berg, O.: Orientation constraints in diffusion-limited macromolecular association. the role of surface diffusion as a rate-enhancing mechanism. Biophys. J. **47**(1), 1–14 (1985)
20. Marchuk, G., Petrov, R., Romanyukha, A., Bocharov, G.: Mathematical model of antiviral immune response. i. Data analysis, generalized picture construction and parameters evaluation for hepatitis b. J. Theor. Biol. **151**(1), 1–40 (1991), cited By 38. https://doi.org/10.1016/S0022-5193(05)80142-0. https://www.scopus.com/inward/record.uri?eid=2-s2.0-0025819779&doi=10.1016
21. Fory's, U.: Marchuk's model of immune system dynamics with application to tumour growth. J. Theor. Med. **4**(1), 85–93 (2002). https://doi.org/10.1080/10273660290052151. http://www.tandfonline.com/doi/pdf/10.1080/10273660290052151. http://www.tandfonline.com/doi/abs/10.1080/10273660290052151
22. Nakonechny, A., Marzeniuk, V.: Uncertainties in medical processes control. Lecture Notes in Economics and Mathematical Systems, vol. 581, pp. 185–192 (2006), cited By 2. https://doi.org/10.1007/3-540-35262-7_11. https://www.scopus.com/inward/record.uri?eid=2-s2.0-53749093113&doi=10.1007
23. Marzeniuk, V.: Taking into account delay in the problem of immune protection of organism. Nonlinear Anal.: Real World Appl. **2**(4), 483–496 (2001), cited By 2. https://doi.org/10.1016/S1468-1218(01)00005-0. https://www.scopus.com/inward/record.uri?eid=2-s2.0-0041331752&doi=10.1016
24. Prindle, A., Samayoa, P., Razinkov, I., Danino, T., Tsimring, L.S., Hasty, J.: A sensing array of radically coupled genetic 'biopixels'. Nature **481**(7379), 39–44 (2011). https://doi.org/10.1038/nature10722
25. Jones, J.H.: Notes on R0. Department of Anthropological Sciences, California (2007)

26. Yang, J., Wang, X., Zhang, F.: A differential equation model of hiv infection of cd t-cells with delay. Discrete Dynamics in Nature and Society, vol. 2008 (2008)
27. Kuang, Y.: Delay Differential Equations with Applications in Population Dynamics. Academic, New York (1993)
28. He, X.-z.: Stability and delays in a predator-prey system. J. Math. Anal. Appl. **198**(2), 355–370 (1996). https://doi.org/10.1006/jmaa.1996.0087
29. Wendi, W., Zhien, M.: Harmless delays for uniform persistence. J. Math. Anal. Appl. **158**(1), 256fffdfffdfffd268 (1991). https://doi.org/10.1016/0022-247x(91)90281-4
30. Lancaster, P., Tismenetsky, M.: The Theory of Matrices: With Applications. Elsevier, Amsterdam (1985)